The cleft lip and palate defects in *Dancer* mutant mice result from gain of function of the *Tbx10* gene

Jeffrey O. Bush*, Yu Lan†, and Rulang Jiang*†‡

*Department of Biology, University of Rochester, Rochester, NY 14627; and †Center for Oral Biology and Department of Biomedical Genetics, University of Rochester School of Medicine and Dentistry, Rochester, NY 14642

Cleft lip and palate (CL/P) is a common disfiguring birth defect with complex, poorly understood etiology. Mice carrying a spontaneous mutation, *Dancer* (*Dc*), exhibit CL/P in homozygotes and show significantly increased susceptibility to CL/P in heterozygotes [Deol, M. S. & Lane, P. W. (1966) *J. Embryol. Exp. Morphol.* 16, 543–558 and Trasler, D. G., Kemp, D. & Trasler, T. A. (1984) *Teratology* 29, 101–104], providing an animal model for understanding the molecular pathogenesis of CL/P. We genetically mapped *Dc* to within a 1-cM region near the centromere of chromosome 19. *In situ* hybridization analysis showed that one positional candidate gene, *Tbx10*, is ectopically expressed in *Dc* mutant embryos. Positional cloning of the *Dc* locus revealed an insertion of a 3.3-kb sequence containing the 5′ region of the *p23* gene into the first intron of *Tbx10*, which causes ectopic expression of a *p23-Tbx10* chimeric transcript encoding a protein product identical to a normal variant of the Tbx10 protein. Furthermore, we show that ectopic expression of *Tbx10* in transgenic mice recapitulates the *Dc* mutant phenotype, indicating that CL/P in *Dc* mutant mice results from the *p23* insertion-induced ectopic *Tbx10* expression. These results identify gain of function of a T-box transcription factor gene as a mechanism underlying CL/P pathogenesis.

Cleft lip with or without cleft palate (CL/P) is a common birth defect that affects ≈1 in 700 live births worldwide (1–3). CL/P patients are born with unilateral or bilateral gaps in the upper lip that often extend through the upper jaw into the nostrils. Approximately 50% of CL/P patients exhibit other major developmental defects, for which >300 syndromes, including a number of chromosomal or Mendelian disorders, have been documented (4). The other 50% of CL/P cases are nonsyndromic and do not exhibit simple Mendelian inheritance patterns (5, 6). Nevertheless, extensive epidemiological studies have provided strong evidence, such as familial aggregation, recurrence risks, and high concordance rates in monozygotic twins, that indicate genetic predisposition to CL/P (7). Due to the genetic heterogeneity and paucity of multiplex families for genetic linkage mapping, many studies have attempted to investigate the genetic basis of CL/P by association studies of genes involved in craniofacial development in animal models (6, 7). Despite intense efforts, however, this approach has been largely unsuccessful and the major genes responsible for CL/P pathogenesis remain elusive.

Although a few human disease syndromes have either CL/P or cleft secondary palate without cleft lip as features (8, 9), genetic and embryological studies indicate that CL/P and isolated cleft palate are etiologically distinct (10, 11). Whereas cleft secondary palate is seen in many mutant mouse strains, only four mouse cleft lip mutations, including *Dancer* (*Dc*) (12), *Twirler* (13, 14), *Brachyphalangy* (15), and *legless* (16), have been reported. *Dc* and *Twirler* are distinct spontaneous mutations in unknown genes and each results in nearly complete penetrance of CL/P in homozygous mutants (12–14). *Brachyphalangy* was a radiation-induced mutation allelic to the *Gli3* gene (15), but the developmental basis of CL/P in the homozygous mutants is not known because several other *Gli3* mutations do not have a CL/P phenotype (17, 18). The *legless* mutation arose from a transgenic insertion that disrupted the *Sp8* gene, resulting in gross limb and brain developmental defects with a low frequency of CL/P apparently as a secondary consequence (19). In addition to these Mendelian mutations, CL/P occurs spontaneously at low but stable frequencies in one family of inbred mouse strains, the "A" strains (20). A genome-wide screen for cleft susceptibility loci in the *A/WySn* strain mapped two interacting recessive loci, *clf1* and *clf2*, that contribute to cleft lip formation (21–23). Understanding the molecular basis of CL/P formation in these mutant mouse strains will provide new insights into the molecular mechanisms of CL/P pathogenesis in humans.

We report here the characterization and positional cloning of the *Dc* gene. *Dc* heterozygous mice exhibit head tossing and circling behavior whereas *Dc* homozygous mutants have CL/P (12). When outcrossed to the C57BL/6 or A/J inbred strains, up to 40% of *Dc* heterozygous mutants also exhibited CL/P (24). Moreover, *Dc* heterozygous mutants showed significantly increased susceptibility to 6-aminonicotinamide-induced CL/P (25). These data indicate that *Dc* predisposes embryos to CL/P and provides a model for investigating gene–gene and gene–environment interactions in CL/P pathogenesis. *Dc* was previously loosely mapped to proximal chromosome 19 (12). Interestingly, a recent genome-wide screen for CL/P susceptibility loci in humans identified the centromeric region of human chromosome 11, which is syntenic to mouse proximal chromosome 19, as having strong linkage to CL/P (26). Here, we show that the *Dc* locus contains a translocation insertion in the *Tbx10* gene, which encodes a member of the T-box family of DNA-binding transcription factors (27, 28). We show that *Dc* causes ectopic expression of a variant *Tbx10* transcript and that ectopic expression of *Tbx10* mRNA results in CL/P in transgenic mice. These data identify a molecular mechanism underlying CL/P pathogenesis.

Methods

Genetic Mapping of the *Dc* Mutation. *Dc* stock mice were obtained from The Jackson Laboratory through rederivation from frozen embryos and were maintained within the stock background by sibling intercrosses. *Dc*/+ stock females were crossed with *CAST/Ei* males and their heterozygous male progeny were then crossed to either wild-type females from the *Dc* stock or *C3H/HeJ* wild-type females. N2 mice were evaluated for heterozygous phenotype and genomic DNA was isolated from tail biopsy samples for PCR genotyping with microsatellite markers. Molecular markers used for mapping include *D19Mit29*, *D19Mit32*, *D19Mit44*, *D19Mit59*, *D19Mit68*, *D19Mit69*, *D19Mit78*, *D19Mit94*, and *FosL1*. We confirmed recombinations between
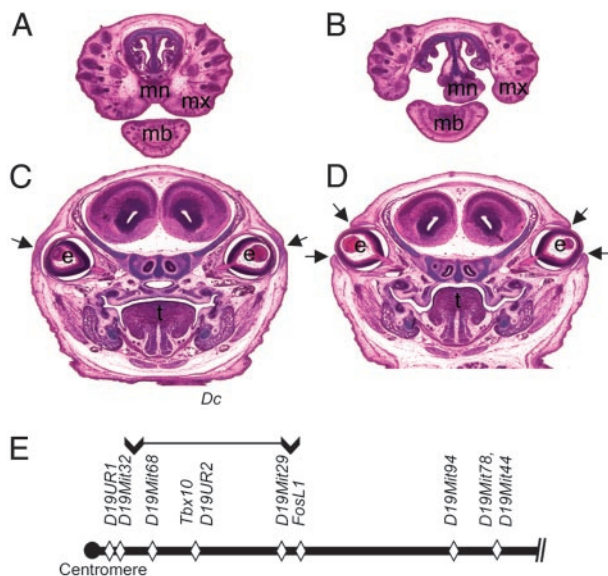
Fig. 1. *Dc/Dc* homozygous mutant mice have cleft lip and palate. (*A–D*) Frontal sections of E16.5 embryonic heads show that *Dc/Dc* homozygotes have bilateral cleft lip (*B*) and cleft palate (*D*). Whereas bilateral secondary palatal shelves have elevated to above the tongue and fused to each other at the midline in wild-type littermates (*C*), palatal shelves failed to elevate in *Dc/Dc* embryos (*D*). *Dc/Dc* homozygotes also exhibited delayed eyelid closure (arrows in *C* and *D*). (*E*) *Dc* was mapped to the centromeric end of chromosome 19. Informative microsatellite markers are shown. The *Dc* locus is mapped between *D19Mit32* and *FosL1*. Markers *D19Mit68*, *D19Mit29*, and *D19UR2* showed no recombination with *Dc* in >500 mice genotyped. e, eye; mb, mandible; mn, medial nasal process; mx, maxilla; t, tongue.

Dc and *D19Mit32* at the centromeric end with a (CA) repeat microsatellite, *D19UR1*, located ≈8.4 kb proximal to *D19Mit32*. The PCR primers for *D19UR1* were 5′-CATACTTCATCAG-GACTTTCATGC-3′ and 5′-GTGCTTCTGGCAGTTCCT-CAG-3′, which amplified a 136-bp fragment from *C3H/HeJ* and *Dc* stock genomic DNA and an ≈126-bp fragment from *CAST/Ei* DNA. PCR primers for *D19UR2*, a marker in the 5′ region of the *Tbx10* gene were 5′-CATGTAGACATGT-

GATCTAGCATG-3′ and 5′-CAGCCCAGATTCTCA-GAAGTG-3′, which amplified a 186-bp fragment from *C3H/HeJ* and *Dc* stock genomic DNA and an ≈170-bp fragment from *CAST/Ei* genomic DNA.

Histology and *in Situ* Hybridization. Embryos were dissected and DNA was prepared from yolk sac or tail samples for genotyping by PCR. Embryos for histology were fixed in Bouin's fixative, dehydrated through graded alcohols, embedded in paraffin, and sectioned and stained with hematoxylin/eosin. Embryos for whole-mount *in situ* hybridization were fixed in 4% paraformaldehyde in PBS overnight at 4°C. The whole-mount *in situ* hybridization protocol and the *Tbx10* probe have been described (28, 29). For comparison of wild-type and *Dc* mutant expression patterns of *Tbx10*, embryos were processed as litters in the same vial, photographs were taken, and embryos were subsequently lysed for PCR genotyping. For negative control, sense RNA probes were used, which did not detect any signal in wild-type or mutant embryos.

RACE and RT-PCR. RACE analysis was carried out by using the GeneRacer kit (Invitrogen) with total RNA isolated from embryonic day (E)11.5 wild-type or *Dc/Dc* embryos. The sequences of 5′ RACE primers were 5′-GCCCGCTTTGGTGA-CAATCATCTCTGT-3′ and 5′-GACTCCTGCCCACCTCT-GCCTTGTG-3′. RT-PCR amplification of *Tbx10* wild-type cDNA was achieved with total RNA from E11.5 mouse embryos by using primers 5′-AATCAGAGGCAGTTTGAGACACC-3′ and 5′-GACATTCGAAGCAGGATTTAGAG-3′. *Dc*-specific *p23-Tbx10* cDNA was amplified by using primers 5′-CAC-CGTTTGTCTGGCCCTCT-3′ and 5′-CAGGGCATGAT-TCAGGGCTTTTG-3′.

Southern Hybridization. Genomic DNA derived from tail samples of *Dc/+* and *+/+* mice was digested with a panel of restriction enzymes individually. After electrophoresis through 1% agarose gels, DNA was transferred onto Zetaprobe GT membranes (Bio-Rad) and hybridized according to the manufacturer's instructions. The *Tbx10* exon 1 probe was an 800-bp *Hin*dIII/*Sph*I fragment of the exon 1 region and the exon 2 probe was a 460-bp *Hin*dIII/*Nco*I fragment from the intron 1/exon 2 junction of the *Tbx10* gene.
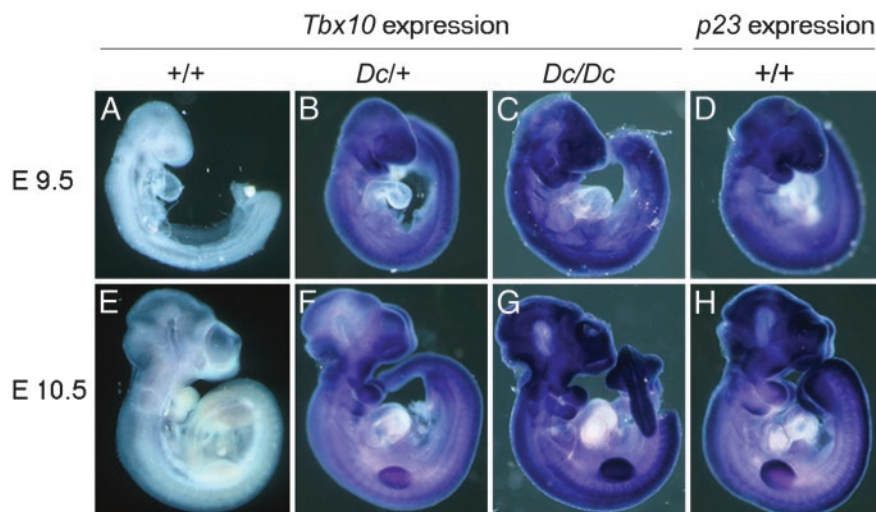

Fig. 2. *Dc* mutant embryos have ectopic *Tbx10* mRNA expression. *In situ* hybridization analysis revealed widespread ectopic overexpression of *Tbx10* at E9.5 (*B* and *C*) and E10.5 (*F* and *G*) in *Dc* mutants compared with the wild-type (*A* and *E*) littermates. Because of the short detection time used due to overexpression of *Tbx10* in mutant embryos, the restricted wild-type *Tbx10* expression pattern in the developing hindbrain is barely visible. (*D* and *H*) The pattern of *p23* mRNA expression in wild-type embryos is very similar to that of the ectopic *Tbx10* expression in *Dc* mutant embryos.

Quantitative Real-Time RT-PCR Analysis of *Tbx10* Expression. Template cDNA was synthesized from total RNA isolated independently from *Dc* mutant and wild-type E11.5 embryos by using the Invitrogen first-strand synthesis kit. Template cDNA was then PCR-amplified in the presence of the fluorogenic DNA dye SYBR Green I by using the Bio-Rad iCycler. Standard curves were generated by a series of 1:10 dilutions of a reference cDNA for each primer pair examined and the expression of each target was then calculated relative to this standard curve. Total *Tbx10* transcripts were quantified by amplifying a 165-bp fragment by using a forward primer (5′-TGCGGCAGATTGTGTCCTTG-3′) corresponding to the exon 4 sequence and a reverse primer (5′-AGTTTTCCTGGGCATAGCGGG-3′) complementary to the exon 5 sequence of *Tbx10*. Wild-type *Tbx10* exon 1-containing transcripts were quantified by using a forward primer (5′-TGCTTGAGAGTGAGGTCTGCTGC-3′) corresponding to the exon 1 sequence and a reverse primer (5′-AGCTGGTGCT-GGTCTCGGG-3′) complementary to the exon 2 sequence to amplify a 200-bp fragment. These transcripts were quantified relative to the expression of hypoxanthine phosphoribosyl-transferase I (*Hprt*) and β-actin mRNAs by using the standard curve method. *Hprt* primers are 5′-TGCTGGTGAAAAGGAC-CTCTCG-3′ and 5′-CTGGCAACATCAACAGGACTCC-3′. β-actin primers are 5′-GGCCGCCCTAGGCACCAG-3′ and 5′-GGGTCATCTTTTCACGGTTGGC-3′.

Generation of Transgenic Mice. Transgenic mice were generated by microinjection of gel-purified, transgenic DNA constructs into the pronuclei of fertilized eggs of *B6SJLF2* mice. The *CMVβ-Tbx10* transgenic construct was generated by cloning the RT-PCR-isolated *p23-Tbx10* cDNA (described above) downstream of the previously described *CMV-β-actin* promoter (30). Transgenic mice were genotyped by using PCR with a *β-actin* forward primer (5′-AGCCTCTGCTAACCAT-3′) and *Tbx10* exon 2 reverse primer (5′-GCCCGCTTTGGTGACAATCATCTCTGT-3′).

Results and Discussion

Genetic Mapping of *Dc* and Identification of *Tbx10* as a Candidate Gene. *Dc* mutant mice were removed from breeding colonies many years ago and the stock embryos were cryopreserved at The Jackson Laboratory. We obtained two presumed *Dc* heterozygous mice with head-tossing behavior rederived from frozen *Dc* stock embryos and established a breeding colony. We found that nearly 25% of newborn progeny from heterozygous intercrosses exhibited cleft lip at birth. Histological analysis of newborn and late gestation embryos showed that cleft lip is always accompanied by cleft palate in the homozygous mutants (Fig. 1 *B* and *D*). In addition, some homozygous mutants exhibited open eyelids at birth (Fig. 1*D*).

To refine the chromosomal location of the *Dc* mutation, we used an intraspecific backcross mapping strategy and genotyped >500 phenotypically heterozygous N2 mutant mouse progeny from [wild-type × (*Dc*/+ × *CAST/Ei*)F1] crosses for microsatellite markers located on proximal chromosome 19. Eleven mice carried informative recombination and were further genotyped with more closely linked markers, which localized the *Dc* mutation to within a 1-cM region near the centromere, between markers *D19Mit32* and *FosL1* (Fig. 1*E*).

Searching the mouse genome databases revealed that the genomic region between *D19Mit32* and *FosL1* spans ≈2.2 Mb of DNA. This region contains >90 predicted transcription units, one of which encodes a member of the T-box family of DNA-binding transcription factors, Tbx10 (27, 28). T-box genes are evolutionarily conserved and play essential roles in many developmental processes throughout metazoans (31, 32). *Tbx10* is closely related to *TBX1* and *TBX22*, two human T-box genes of which loss of function causes cleft palate associated with Di-George Syndrome and X-linked cleft palate with ankyloglossia,
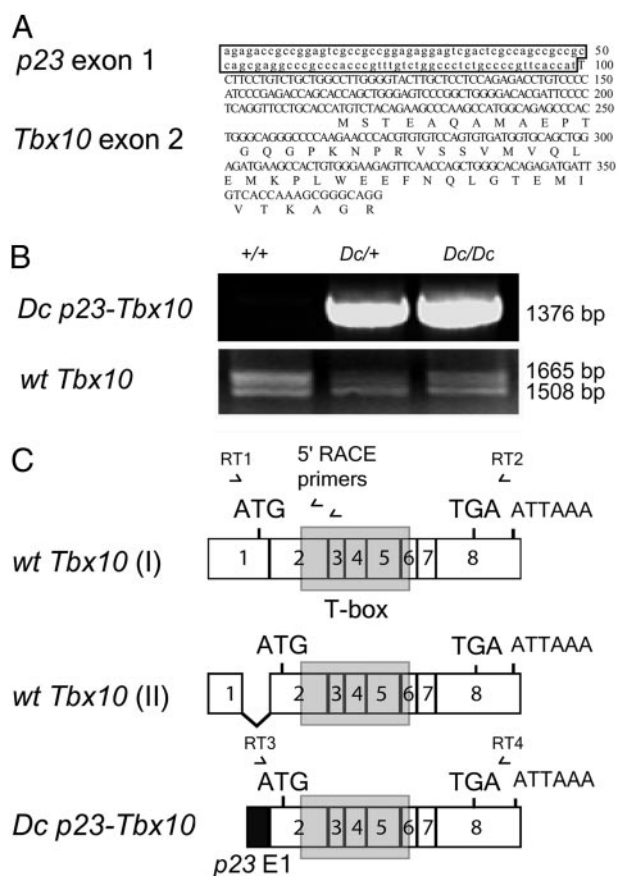

Fig. 3. *Dc* mutant embryos express a *p23-Tbx10* chimeric transcript. (*A*) Sequence analysis of 5′ RACE products showed that the majority of *Tbx10* transcripts in *Dc* mutants have their exon 1 sequence replaced by 99 nucleotides from the first exon of the *p23* gene. The *p23* nucleotide sequence is shown in lowercase and the *Tbx10* exon 2 sequence in uppercase. Translation of the chimeric transcript is predicted to initiate in the *Tbx10* exon 2 sequence. (*B*) RT-PCR analysis confirmed expression of *p23-Tbx10* chimeric transcripts in *Dc*/+ and *Dc*/*Dc* mutant embryos and revealed expression of two different-sized wild-type *Tbx10* transcripts. (*C*) Schematic representation of wild-type and *Dc Tbx10* cDNAs. Numbers in the boxes indicate exons. The positions of predicted translation start (ATG) and stop (TGA) codons are marked. Polyadenylation signals (ATTAAA) are also indicated. Positions of the primers used for RT-PCR are marked. Sequence analysis of RT-PCR products shown in *B* showed that the two different wild-type *Tbx10* transcripts result from alternative splicing in exon 1. The mutant *p23-Tbx10* chimeric transcript is predicted to encode a protein truncated by 41 amino acids in the N terminus compared with the full-length protein predicted from the long isoform of wild-type *Tbx10* mRNA, *wt Tbx10* (*I*), but identical to that encoded by the shorter wild-type splice variant, *wt Tbx10* (*II*).

respectively (33, 34). Targeted disruption of *Tbx1* also caused cleft palate in mice (35). To verify the close linkage between *Tbx10* and *Dc*, we identified a polymorphic microsatellite sequence, D19UR2, located in the 5′ region of the *Tbx10* gene and genotyped all DNA samples of our *Dc*-mapping mice with this marker. No recombination between D19UR2 and *Dc* was observed in >500 mice genotyped, suggesting that *Tbx10* is a strong candidate for the *Dc* gene.

We investigated the *Tbx10* expression pattern during normal craniofacial development. Extensive *in situ* hybridization analysis showed that *Tbx10* mRNA is expressed in a highly restricted pattern in the developing hindbrain and is normally not expressed in the developing facial region (Fig. 2 *A* and *E* and ref. 28), suggesting that loss of function of *Tbx10* was unlikely to result in CL/P. Moreover, we sequenced PCR fragments covering all eight exons and exon/
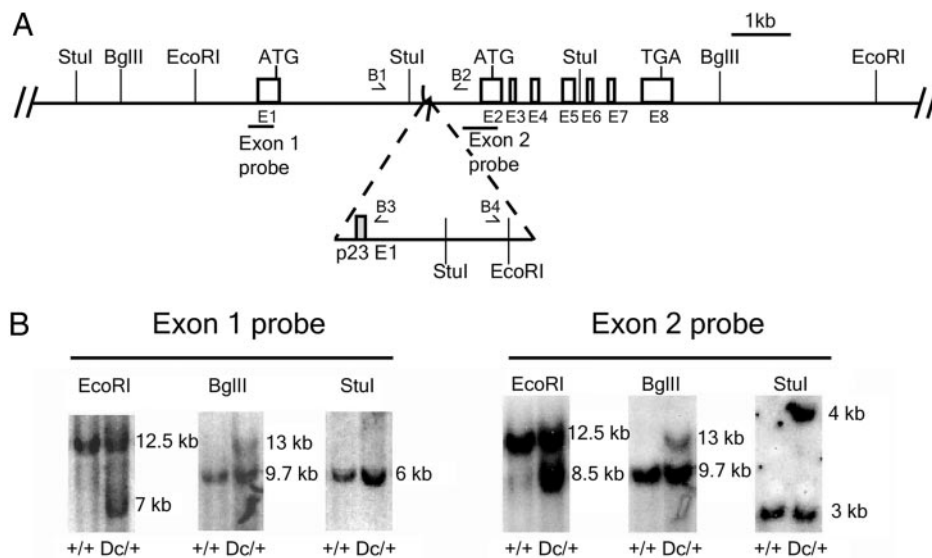
Bush *et al.*

Fig. 4. The *Dc* locus contains an insertion of the 5′ region of the *p23* gene in the first intron of *Tbx10*. (*A*) Schematic of the *Dc* mutant locus indicating insertion of a 3.3-kb fragment containing the *p23* exon 1 in the first intron of *Tbx10*. The *Tbx10* exons are labeled E1–E8. The ATG codons in E1 and E2 correspond to the translation start sites of the alternatively spliced wild-type *Tbx10* mRNAs, respectively. Recognition sites for the restriction enzymes *Bgl*II, *Eco*RI, and *Stu*I are marked. Positions of PCR primers used to amplify the mutant genomic fragments are labeled as B1–B4. The genomic regions corresponding to the exon 1 and exon 2 probes used for Southern hybridization are also indicated. (*B*) Southern hybridization analysis of genomic DNA isolated from +/+ and *Dc*/+ mutant mice. The sizes of the hybridized fragments are marked to the right of each image.

intron boundaries of the *Tbx10* gene amplified from *Dc*/*Dc* mutant DNA but did not find any mutation.

Because the *Dc* mutation is semidominant, we hypothesized that *Dc* might be a neomorphic regulatory mutation in the *Tbx10* gene. T-box genes are known to be dose-sensitive and overexpression of several T-box transcription factors resulted in various developmental consequences (36, 37). In particular, transgenic mice carrying a BAC construct containing the human *TBX1* gene displayed hyperactive head-tilting behavior, which resembled the *Dc*/+ heterozygous phenotype (38). We therefore investigated whether *Tbx10* mRNA expression was altered in *Dc* mutant embryos. *In situ* hybridization analysis revealed widespread ectopic *Tbx10* mRNA expression in approximately three-quarters of *Dc*/+ intercross progeny from E9 through E12, with strong ectopic expression in the first pharyngeal arches and the limb buds, whereas the remaining embryos expressed *Tbx10* in the highly restricted wild-type pattern as reported (28). Genotyping the embryos confirmed that ectopic *Tbx10* mRNA expression is specific to the *Dc*/+ and *Dc*/*Dc* mutant embryos (Fig. 2), indicating that *Dc* causes misregulation of the *Tbx10* gene.

The *Dc* Locus Contains an Insertion in the First Intron of *Tbx10*. To investigate the cause of ectopic *Tbx10* expression in *Dc* mutants, we carried out 5′ RACE analysis by using reverse primers corresponding to either the exon 2 or exon 3 sequences of the *Tbx10* gene (Fig. 3). Sequence analysis of the 5′ RACE products indicated that the majority of *Tbx10* transcripts in *Dc* mutant embryos have the *Tbx10* exon 1 sequence replaced by a 99-nt sequence identical to the 5′ UTR of the *p23* mRNA (Fig. 3*A*). RT-PCR analysis of E11.5 embryonic RNA confirmed expression of *p23-Tbx10* chimeric transcripts specifically in *Dc*/+ and *Dc*/*Dc* mutant embryos (Fig. 3 *B* and *C*). Because the *p23* sequence in the chimeric transcript does not contain an AUG codon, translation of the *p23-Tbx10* chimeric transcript is predicted to initiate within the *Tbx10* exon 2 sequence and to produce a protein with an intact T-box domain but lacking the N-terminal 41-aa residues of the previously reported Tbx10 protein (Fig. 3*C*). Interestingly, RT-PCR analysis showed that

wild-type embryos express *Tbx10* transcripts of two different sizes (Fig. 3*B*). Sequence analysis showed that the longer RT-PCR product corresponds to the previously reported *Tbx10* cDNA (37), whereas the shorter product corresponds to an alternatively spliced *Tbx10* mRNA that lacks sequences from the 3′ half of exon 1 (GenBank accession no. AY542280). This alternatively spliced shorter *Tbx10* mRNA is predicted to encode a protein product identical to that of the *p23-Tbx10* chimeric transcripts (Fig. 3*C*).

Searching the mouse genome databases revealed that the *p23* gene is located on mouse chromosome 10 and the *p23* sequence in the *p23-Tbx10* chimeric transcript corresponds to the exon 1 sequence of the *p23* gene. Thus, the *Dc* mutation resulted most likely from a translocation insertion of a chromosome 10 segment containing at least part of the *p23* gene into the vicinity of the *Tbx10* gene on chromosome 19. *In situ* hybridization analysis showed that *p23* mRNA expression patterns in wild-type embryos matched the ectopic *Tbx10* expression patterns in *Dc* mutant embryos (Fig. 2), suggesting that expression of the *p23-Tbx10* chimeric mRNA in *Dc* mutant embryos is driven by the *p23* gene promoter.

To identify the insertion breakpoints at the *Dc* locus, we carried out Southern hybridization analyses by using genomic DNA fragments corresponding to the exon 1 and exon 2 regions of the *Tbx10* gene as probes. Both probes detected distinct-sized mutant-specific *Eco*RI fragments that were smaller than the wild-type *Eco*RI fragment (Fig. 4*B*), indicating that the *p23* fragment is inserted into the first intron. Hybridization of the two probes to *Stu*I-digested wild-type and *Dc*/+ DNA samples further localized the insertion site to within a 1.2-kb region between the *Stu*I site in intron 1 and exon 2 (Fig. 4).

According to the mouse genome database annotation, the *p23* gene is composed of eight exons spanning ≈22 kb of genomic DNA, with the first intron being ≈9.4 kb in size. Because the *p23-Tbx10* chimeric transcript only contained the exon 1 sequences of the *p23* gene, we investigated the possibility that the 3′ end of the insertion may lie in intron 1 of the *p23* gene. We paired forward PCR primers corresponding to sequences in intron 1 of the *p23* gene with reverse primers from the exon 2
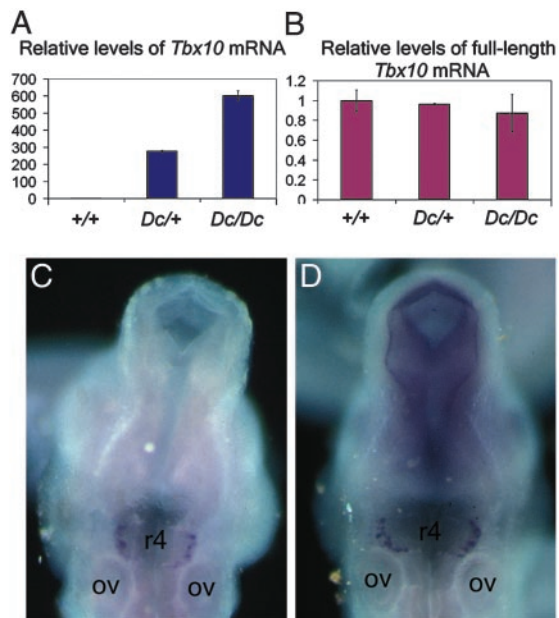
Fig. 5. Full-length *Tbx10* mRNA is expressed normally in *Dc* mutant embryos. (*A*) Quantitative real-time RT-PCR by using *Tbx10* primers corresponding to sequences of the fourth and fifth exons showed a dramatic overexpression of *Tbx10* transcripts in E11.5 *Dc*/+ and *Dc*/*Dc* mutant embryos compared with wild-type (+/+) littermates. (*B*) Quantitative real-time RT-PCR by using primers corresponding to sequences of the first and second exons showed no significant difference in expression levels of full-length *Tbx10* mRNA between +/+, *Dc*/+, and *Dc*/*Dc* embryos. Error bars represent SD. (*C* and *D*) *In situ* hybridization analysis by using an cRNA probe specific to the *Tbx10* exon 1 sequence showed that full-length *Tbx10* mRNA expression is highly restricted to the fourth rhombomere in *Dc*/+ (*C*) and *Dc*/*Dc* (*D*) embryos at E10.5, which is indistinguishable from the expression pattern in +/+ embryos. ov, otic vesicle; r4, fourth rhombomere.

region of the *Tbx10* gene and attempted PCR amplification across the 3′ insertion break point in *Dc*/*Dc* homozygous mutant DNA. Sequence analysis of PCR-amplified fragments indicated that the insertion contained exon 1 and the first 2,995 bp of intron 1 of the *p23* gene and was inserted at 917 bp 5′ to exon 2 of *Tbx10* (Fig. 4*A*).

Southern hybridization analysis also provided information for estimating the size of the insertion. As shown in Fig. 4*B*, the exon 1 and exon 2 probes both detected an ≈13-kb mutant-specific *Bgl*II fragment, which is ≈3.3 kb larger than the wild-type *Bgl*II fragment. Analysis of the *p23* gene region indicated the presence of a *Bgl*II site ≈270 bp upstream of the 99-bp *p23* exon 1 sequence. If the *Dc* locus contained this *Bgl*II site, however, the exon 2 probe would be expected to detect a mutant-specific *Bgl*II fragment of ≈8 kb in size. The absence of this predicted *Bgl*II site at the *Dc* locus suggested that the 5′ end of the insertion is probably downstream of this *Bgl*II site in the *p23* promoter region. We tested this possibility by PCR amplification across the predicted 5′ end of the insertion. Sequence analysis of PCR products showed that the entire insertion contained a 3,328-bp fragment of the *p23* gene region, from 234 bp upstream of the 99-bp exon 1 to 2,995 bp into intron 1 (Fig. 4*A*). This insertion did not cause any deletion of *Tbx10* sequence (data not shown).

The *Dc* mutation, while causing ectopic expression of the *p23*-*Tbx10* chimeric transcripts, did not alter the expression levels of the full-length *Tbx10* transcripts (Fig. 5*B*). The highly restricted expression pattern of the full-length *Tbx10* mRNA was also maintained in *Dc*/+ and *Dc*/*Dc* mutant embryos (Fig. 5 *C* and *D*). We performed quantitative real-time RT-PCR analyses of mRNA expression of four other genes in the vicinity of *Tbx10*
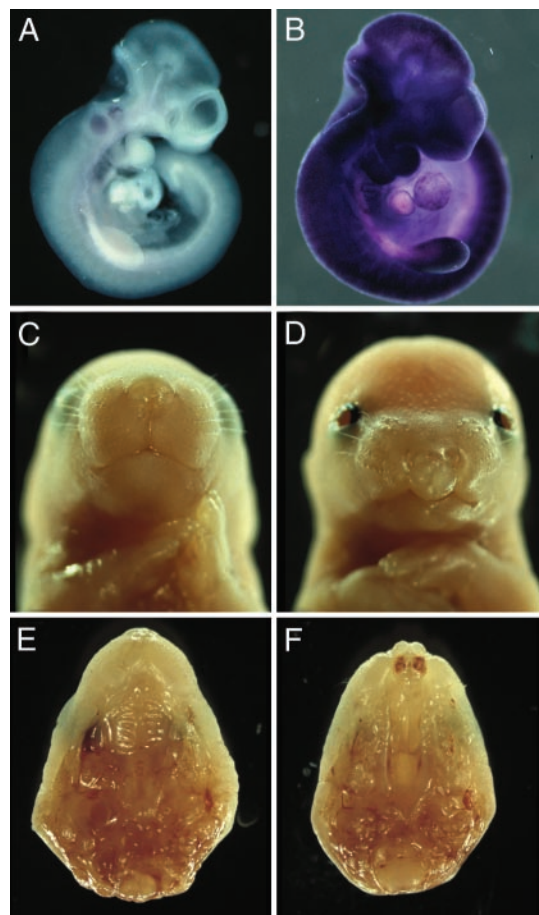

Fig. 6. Transgenic *Tbx10* overexpression causes CL/P. (*A* and *B*) Whole-mount *in situ* hybridization analysis showed ubiquitous overexpression of *Tbx10* transcripts in *CMVβ-Tbx10* transgenic embryos at E10.5 (*B*) compared with the highly restricted hindbrain expression in wild-type littermates (*A*). (*C* and *D*) Frontal views of a wild-type E18.5 embryo (*C*) and of a littermate transheterozygous for *Dc* and the *CMVβ-Tbx10* transgene (*D*). The transheterozygous embryo exhibited bilateral cleft lip and open eyelids. (*E* and *F*) Palatal views of wild-type (*E*) and transheterozygous mutant (*F*) upper jaws showed cleft primary and secondary palates in the mutant.

but did not find any alterations in *Dc*/*Dc* mutant embryos (data not shown), indicating that the *p23* insertion did not disrupt other genes at the *Dc* locus.

Ectopic Expression of *Tbx10* in Transgenic Mice Recapitulates the *Dc* Mutant Phenotypes. We next investigated whether ectopic *Tbx10* expression causes the *Dc* mutant phenotype. We generated transgenic mice expressing the *p23*-*Tbx10* chimeric transcripts by using the *CMVβ* promoter (30). Three transgenic founder mice survived to adulthood, of which one male founder transmitted the transgene through the germ line. Whole-mount *in situ* hybridization analysis of embryos collected from wild-type females mated with this transgenic founder male showed that the *Tbx10* transgene was expressed throughout hemizygous transgenic embryos (Fig. 6*B*). Breeding the transgenic founder male with wild-type females of the *Dc* stock generated six surviving hemizygous transgenic progeny, which all exhibited head-tossing behavior that resembled the *Dc*/+ mutant mice. Examination of two litters of newborn pups found two hemizygous transgenic progeny with CL/P and open eyelids (data not shown). Crossing F1 transgenic hemizygotes with *Dc*/+ heterozygous mice resulted in three transheterozygous mutants, which all exhibited CL/P and open eyelids at birth (Fig. 6 *D* and *F*), whereas none

of the $Dc/+$ heterozygous littermates that did not carry the transgene exhibited CL/P. In addition, breeding $Dc/+$ heterozygous stock mice with the nontransmitting transgenic founders yielded >20 $Dc/+$ heterozygous progeny, none of which had CL/P. That some hemizygous transgenic mice exhibited CL/P, whereas $Dc/+$ heterozygous mice did not in the transgenic strain background, is likely due to higher levels of *Tbx10* mRNA overexpression from the transgenes. The fact that ectopic expression of *Tbx10* mRNA by using a heterologous promoter different from that in the *Dc* locus is sufficient to recapitulate both the heterozygous and homozygous phenotypes of the *Dc* mutation indicates that the *Dc* mutant phenotypes result from ectopic *Tbx10* expression induced by the *p23* insertion.

Several possibilities exist for the action of ectopic *Tbx10* in *Dc* embryos. The ectopically expressed Tbx10 protein may directly activate or repress downstream target genes, resulting in disturbance of craniofacial development. In both *Dc* mutant mice and the *CMVβ-Tbx10*-transgenic mice, *Tbx10* mRNA is expressed nearly ubiquitously, but the developmental defects are highly specific to the craniofacial region. This finding suggests that the downstream effects of transcriptional modulation of any target gene may be highly specific to the developing craniofacial region. Alternatively, ectopic Tbx10 expression may antagonize the function of other closely related T-box factors, such as Tbx1, Tbx15, Tbx18, and Tbx22, which all share high amino acid sequence identity in their DNA-binding domains and are all expressed in partially overlapping patterns during craniofacial development (39–43). Mutations in *Tbx1* and *TBX22* cause craniofacial defects that include cleft palate in mice and humans, respectively (34, 35). A recent study in zebrafish (44) showed that closely related T-box transcription factors can interact either synergistically or antagonistically to regulate region specific developmental fate in overlapping expression domains. Further investigation of *Tbx10* function in *Dc* mutants will lead to a better understanding of the molecular pathways involved in craniofacial development and CL/P pathogenesis. Interestingly, a recent genome-wide scan of CL/P susceptibility loci in humans identified strong linkage with the centromeric chromosome 11 region where *TBX10* resides (26). It is possible that gain of function of *TBX10* may underlie a subset of CL/P cases in humans.

1. Vanderas, A. P. (1987) *Cleft Palate J.* **24,** 216–225.
2. Tolarova, M. M. & Cervenka, J. (1998) *Am. J. Med. Genet.* **75,** 126–137.
3. Croen, L. A., Shaw, G. M., Wasserman, C. R. & Tolarova, M. M. (1998) *Am. J. Med. Genet.* **79,** 42–47.
4. Gorlin, R. J., Cohen, M. M., Jr., & Hennekam, R. C. M. (2001) in *Syndromes of the Head and Neck* (Oxford Univ. Press, New York), pp. 850–976.
5. Shutte, B. C. & Murray, J. C. (1999) *Hum. Mol. Genet.* **8,** 1853–1859.
6. Murray, J. C. (2002) *Clin. Genet.* **61,** 248–256.
7. Prescott, N. J., Winter, R. M. & Malcolm, S. (2001) *Ann. Hum. Genet.* **65,** 505–515.
8. Kondo, S., Shutte, B. C., Richardson, R. J., Bjork, B. C., Knight, A. S., Watanabe, Y., Howard, E., de Lima, R. L., Daack-Hirsch, S., Sander, A., *et al.* (2002) *Nat. Genet.* **32,** 285–289.
9. van den Boogaard, M. J., Dorland, M., Beemer, F. A. & van Amstel, H. K. (2000) *Nat. Genet.* **24,** 342–343.
10. Diehl, S. R. & Erickson, R. P. (1997) *Proc. Natl. Acad. Sci. USA* **94,** 5231–5236.
11. Wilkie, A. O. & Morriss-Kay, G. M. (2001) *Nat. Genet. Rev.* **2,** 458–468.
12. Deol, M. S. & Lane, P. W. (1966) *J. Embryol. Exp. Morphol.* **16,** 543–558.
13. Lyon, M. F. (1958) *J. Embryol. Exp. Morphol.* **6,** 105–116.
14. Gong, S.-G., White, N. J. & Sakasegawa, A. Y. (2000) *Arch. Oral Biol.* **45,** 87–94.
15. Johnson, D. R. (1969) *Genet. Res.* **13,** 275–280.
16. McNeish, J. D., Scott, W. J., Jr., & Potter, S. S. (1988) *Science* **241,** 837–839.
17. Johnson, D. R. (1967) *J. Embryol. Exp. Morphol.* **17,** 543–558.
18. Vortkamp, A., Franz, T., Gessler, M. & Grzeschik, K. H. (1992) *Mamm. Genome* **3,** 461–463.
19. Bell, S. M., Schreiner, C. M., Waclaw, R. R., Campbell, K., Potter, S. S. & Scott, W. J. (2003) *Proc. Natl. Acad. Sci. USA* **100,** 12195–12200.
20. Kalter, H. (1979) *Teratology* **20,** 213–232.
21. Juriloff, D. M. (1995) *J. Craniofac. Genet. Dev. Biol.* **15,** 1–12.
22. Juriloff, D. M. & Mah, D. G. (1995) *Mamm. Genome* **6,** 63–69.
23. Juriloff, D. M., Harris, M. J. & Brown, C. J. (2001) *Mamm. Genome* **12,** 426–435.
24. Trasler, D. G. & Leong, S. (1982) *Teratology* **27,** 259–265.
25. Trasler, D. G., Kemp, D. & Trasler, T. A. (1984) *Teratology* **29,** 101–104.
26. Prescott, N. J., Lees, M. M., Winter, R. M. & Malcolm, S. (2000) *Hum. Genet.* **106,** 345–350.
27. Law, D. J., Garvey, N., Agulnik, S. I., Perlroth, V., Hahn, O. M., Rhinehart, R. E., Gebuhr, T. C. & Silver, L. M. (1998) *Mamm. Genome* **9,** 397–399.
28. Bush, J. O., Maltby, K. M., Cho, E.-S. & Jiang, R. (2003) *Gene Expr. Patterns* **3,** 533–538.
29. Jiang, R., Lan, Y., Norton, C. R., Sundberg, J. P. & Gridley, T. (1998) *Dev. Biol.* **198,** 277–285.
30. Niwa, H., Yamamura, K. & Miyazaki, J. (1991) *Gene* **108,** 193–199.
31. Papaioannou, V. E. & Silver, L. M. (1998) *BioEssays* **20,** 9–19.
32. Papaioannou, V. E. (2001) *Int. Rev. Cytol.* **207,** 1–70.
33. Merscher, S., Funke, B., Epstein, J. A., Heyer, J., Puech, A., Lu, M. M., Xavier, R. J., Demay, M. B., Russell, R. G., Factor, S., *et al.* (2001) *Cell* **104,** 619–629.
34. Braybrook, C., Doudney, K., Marcano, A. C., Arnason, A., Bjornsson, A., Patton, M. A., Goodfellow, P. J., Moore, G. E. & Stanier, P. (2001) *Nat. Genet.* **29,** 179–183.
35. Jerome, L. A. & Papaioannou, V. E. (2001) *Nat. Genet.* **27,** 286–291.
36. Hatcher, C. J. & Basson, C. T. (2001) *Nat. Med.* **7,** 1185–1186.
37. Takeuchi, J. K. (2003) *Development (Cambridge, U.K.)* **130,** 2729–2739.
38. Funke, B., Epstein, J. A., Kochila, L. K., Lu, M. M., Pandita, R. K., Liao, J., Bauerndistel, R., Schuler, T., Schorle, H., Brown, M. C., *et al.* (2001) *Hum. Mol. Genet.* **10,** 2549–2556.
39. Chapman, D. L., Garvey, N., Hancock, S., Alexiou, M., Agulnik, S. I., Gibson-Brown, J. J., Cebra-Thomas, J., Bollag, R. J., Silver, L. M. & Papaioannou, V. E. (1996) *Dev. Dyn.* **206,** 379–390.
40. Agulnik, S. I., Papaioannou, V. E. & Silver, L. M. (1998) *Genomics* **51,** 68–75.
41. Kraus, F., Haenig, B. & Kispert, A. (2001) *Mech. Dev.* **100,** 83–86.
42. Bush, J. O., Lan, Y., Maltby, K. M. & Jiang, R. (2002) *Dev. Dyn.* **225,** 322–326.
43. Braybrook, C., Lisgo, S., Doudney, K., Henderson, D., Marcano, A. C., Strachan, T. A., Patton, M. A., Villard, L., Moore, G. E., Stanier, P., *et al.* (2002) *Hum. Mol. Genet.* **11,** 2793–2804.
44. Goering, L. M., Hoshijima, K., Hug, B., Bisgrove, B., Kispert, A. & Grunwald, D. J. (2003) *Proc. Natl. Acad. Sci. USA* **100,** 9410–9415.

GENETICS